

Electrochemical Preparation and Characterization of MnO₂-PEDOT Hybrid Film and its Application in Electrocatalytic Oxidation of Memantine Hydrochloride

Zhi-Yuan Wu, Soundappan Thiagarajan, Shen-Ming Chen^{*}, Kuo-Chiang Lin

Electroanalysis and Bioelectrochemistry Lab, Department of Chemical Engineering and Biotechnology, National Taipei University of Technology, No.1, Section 3, Chung-Hsiao East Road, Taipei 106, Taiwan (ROC).

*E-mail: smchen78@ms15.hinet.net

Received: 12 December 2011 / Accepted: 2 January 2012 / Published: 1 February 2012

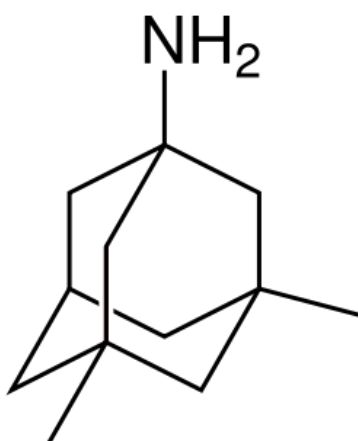
The MnO₂-PEDOT hybrid film had been successfully constructed on electrode surface by cyclic voltammetry. This composite was surface-confined on electrode surface. The MnO₂-PEDOT hybrid film was found to be electrochemically active and stable in pH 7 PBS solution. Morphology study of MnO₂-PEDOT film (3307 nm×3307 nm) was found as the roughness average (R_a) of 7.04 nm, the root mean square roughness (R_{RMS}) of 9.04 nm, The positive skewness value (0.04) obtained for the MnO₂-PEDOT film showed that the surface comprised of disproportionate number of peaks which indicated that the MnO₂ particles were unevenly allocated on the GCE surface. A centrally distributed surface had a kurtosis value greater than 3. In this film, the kurtosis value was found as 3.44. The maximum number of MnO₂ particles had been found in the size range of 258 nm. The electron transfer was a slow process at the MnO₂-PEDOT film modified GCE. The proposed composite showed lower overpotential and higher current response to memantine and hydrogen peroxide as compared with bare electrode. The electrocatalytic oxidation current to memantine and hydrogen peroxide was found linearly in the range of 20–100 μM and 10-140 μM. The linear regressed equation can be expressed as $I_{pa}(\mu A) = 0.019C(\mu M) + 0.543$ and $I_{pa}(\mu A) = 18C(\mu M) + 1.698$ for memantine and hydrogen peroxide, respectively.

Keywords: MnO₂, 3,4-ethylenedioxythiophene, memantine, hydrogen peroxide, electroanalysis, electrochemistry, electrocatalysis

1. INTRODUCTION

Memantine is the first in a novel class of Alzheimer's disease (AD) medications acting on the glutamatergic system by blocking N-methyl-D-aspartate (NMDA) receptors. Memantine has been

associated with a moderate decrease in clinical deterioration in AD [1]. AD is a severe neurodegenerative illness affecting more and more aging population over the world. AD represents the most common cause of dementia and is characterized by a progressive, but irreversible deterioration of cognitive functions and a loss of memory [2]. Although the mechanisms leading to these dysfunctions are still unclear and under debate [3-5], the disease is physiologically characterized by two main pathological features. These hallmarks are: (i) the intracellular accumulation of the hyperphosphorylated tau protein in the neurons and (ii) the progressive production and aggregation of β -amyloid peptide ($A\beta$) [6,7], the latter being considered as the main cause of AD [8]. A systematic review of randomized controlled trials found that memantine has a small positive effect on cognition, mood, behavior, and the ability to perform daily activities in moderate to severe AD, but an unknown effect in mild to moderate disease [9].



Scheme 1. Chemical structure of memantine

Previously different types of analytical techniques have been employed for the detection of memantine hydrochloride. They are, simultaneous liquid chromatographic assay of amantadine and its four related compounds in phosphate-buffered saline using 4-fluoro-7-nitro-2,1,3-benzoxadiazole as a fluorescent derivatization reagent [10], electrophoretic behavior of adamantane derivatives possessing antiviral activity and their determination by capillary zone electrophoresis with indirect detection [11], pharmacokinetics of single-dose and multiple-dose memantine using an analytic method of liquid chromatography-tandem mass spectrometry [12] and determination of memantine in human plasma by liquid chromatography–electro spray tandem mass spectrometry [13] were reported. Above these methods possess good capability for the detection and determination of memantine hydrochloride. However, those methods need much complicated procedure to analyze the memantine. Therefore simple and elegant method is expected for the direct determination of memantine hydrochloride. In electrochemistry, film modified electrodes are found to be effective for the detection and determination of biomolecules and biologically important compounds. Various types of film modified electrodes were successfully reported for the detection of biologically important compounds [14-16].

Hydrogen peroxide (H_2O_2) has been used as antiseptic and antibacterial agent for many years due to its oxidizing effect. It was used by hospitals, doctors, and dentists in sterilizing, cleaning, and

treating everything from floors to root canal procedures. Further H_2O_2 acts as a powerful oxidizing agent, so it could be applied in so many organic compound synthesis reactions [17]. The biological systems will be directly affected by hydrogen peroxide; therefore, the central nervous system diseases could be formed [18]. According to these reasons, there is a need of a sensor to detect the H_2O_2 in clinical and environmental applications [19]. Further the detection and determination of H_2O_2 can be done in several methods like spectrophotometric [20], titrimetric [21], fluorescence [22], phosphorescence [23] and chromatographic methods [24]. Although these methods exhibit obvious result for the determination of H_2O_2 , they still have their own technical drawbacks and some of them were quite expensive. Generally in electrochemical analysis, the reduction or oxidation of hydrogen peroxide is not applicable at bare electrodes. At the bare electrode, it shows the slow electrode kinetics and high over-potential required for this redox reaction. To overcome this problem, the modified electrodes have been widely applied [25]. Further the modified electrodes have shown interesting ability toward hydrogen peroxide detection. But they exhibited with many problems linked to the film deposition process, its toxicity, poor repeatability, and stability. Also the sensitivity of the modified electrodes was restricted to micro-molar concentrations. For these reasons, there is a need to develop simple and reliable methods for fabrication of novel sensor for hydrogen peroxide detection at nano-molar or in lower concentration range.

Oxide nanomaterials modified electrodes keen special interest in electroanalytical chemistry [26, 27]. For example, manganese oxides and hydroxides are of considerable importance in many technological applications. To mention a few, Mn_2O_3 , Mn_3O_4 and MnO_2 have been reported to be efficient catalysts in many environmental reactions and in the synthesis of organic compounds, whereas MnO_2 electrodes are widely used in alkaline batteries [28, 29] in which MnOOH is produced during the electrochemical processes [29]. Further the advantages of using manganese oxides powdered materials with controlled particle size and shape have been amply documented. The properties of such solids can also be altered if the particle size is reduced to the nanometer range. Further the use of conducting polymers (CPs) as modifying materials of the electrode surfaces is till now, far from attracting the interest they deserve, despite the results recently obtained [30, 31]. The advantages of such modifiers are ascribed to efficient anti-fouling and also electrocatalytic effects [32, 33], which are of high meaning just in real matrices. Among the CPs used as modifying materials for electrodes, poly(3,4-ethylenedioxythiophene) (PEDOT) has recently attracted much attention of the electrochemical community, thanks to several advantageous characteristics. Therefore the combination of MnO_2 and conducting polymer such like PEDOT will result in the fabrication of interesting metal oxide-polymer hybrid film which possesses the good electrocatalytic activities. MnO_2 is one of the most popular electrochemical energy storage materials because of its high energy density, low cost, environmental friendliness, and natural abundance [34, 35], but it has poor conductivity [36]. PEDOT has merits of excellent conductivity, high stability, and mechanical flexibility [37], but it provides low electrochemical energy density. Electrodeposition is used here because it is a simple yet versatile method in controlling structures [38-47] and their composition by tuning applied potentials and electrolyte ingredients [38-47].

In this chapter, we report the electrochemical deposition of MnO_2 -PEDOT hybrid film at GCE and ITO. The surface morphological analysis of the proposed film was done by atomic force

microscopy (AFM) technique. Further the electrochemical properties, stability, pH effect, and electrocatalytic reaction of the proposed film were evaluated. The proposed film modified GCE was investigated for the electrocatalytic oxidation reaction of memantine hydrochloride and H_2O_2 , respectively.

2. EXPERIMENTAL

2.1. Reagents

3,4-ethylenedioxythiophene (EDOT) was purchased from Sigma-Aldrich (USA). All other chemicals (Merck) including manganese(II) acetate and hydroxypropyl- β -cyclodextrin were of analytical grade (99%). Double distilled deionized water (DDDW) was used to prepare all the solutions. Such as pH 1 (0.1 M H_2SO_4) was prepared using sulfuric acid to dilute with DDDW. A pH 4 buffer solution was prepared using potassium hydrogen phthalate (0.1 M KHP). A phosphate buffer solution (PBS) of pH 7 was prepared using Na_2HPO_4 (0.05 M) and NaH_2PO_4 (0.05 M). Other higher pH buffer solutions were appropriately adjusted with di-sodium tetraborate, sodium carbonate, and sodium hydroxide, respectively.

2.2. Apparatus

All electrochemical experiments were performed using CHI 1205a potentiostats (CH Instruments, USA). The BAS glassy carbon electrode (GCE) with a diameter of 0.3 cm and exposed geometric surface area of 0.07 cm^2 (purchased from Bioanalytical Systems, Inc., USA) was used. A conventional three-electrode system was used which consists of an Ag/AgCl (3 M KCl) as a reference electrode, a GCE as a working electrode, and a platinum wire as a counter electrode. For the rest of the electrochemical studies, an Ag/AgCl (3 M KCl) was used as a reference. Prior to the experiments, the glassy carbon electrode was ultrasonicated in DDDW for 1 min after finishing the polish by Buehler felt pads and alumina power ($0.05 \mu\text{m}$).

The morphological characterization of hybrid film was examined by means of AFM (Being Nano-Instruments CSPM-4000, China). The AFM image was recorded with multimode scanning probe microscope. Indium tin oxide (ITO) glass was the substrate coated with proposed film for AFM analysis. The buffer solution was entirely altered by deaerating with nitrogen gas atmosphere. The electrochemical cells were kept properly sealed to avoid the oxygen interference from the atmosphere.

3. RESULTS AND DISCUSSION

3.1. Electrochemical preparation and characterization of MnO_2 -PEDOT/GCE

Fig. 1 shows the electrochemical fabrication of MnO_2 -PEDOT hybrid film using consecutive CV between suitable potentials (-0.6 to 1 V) in aqueous H_2SO_4 solution 0.1 M LiClO_4 aqueous solution

containing 5×10^{-3} M hydroxypropyl- β -cyclodextrin, 0.01 M EDOT, and 0.1 M manganese(II) acetate. In the first scan cycle between -0.6 V and 1 V, one anodic peak was found at about 0.7 V and one cathodic peak was found at about 0.3 V depicted the redox process of manganese. Current development was obviously found at these two redox peaks as increasing scan cycles. Particularly, the cathodic peak was positive-shifted to about 0.95 V.

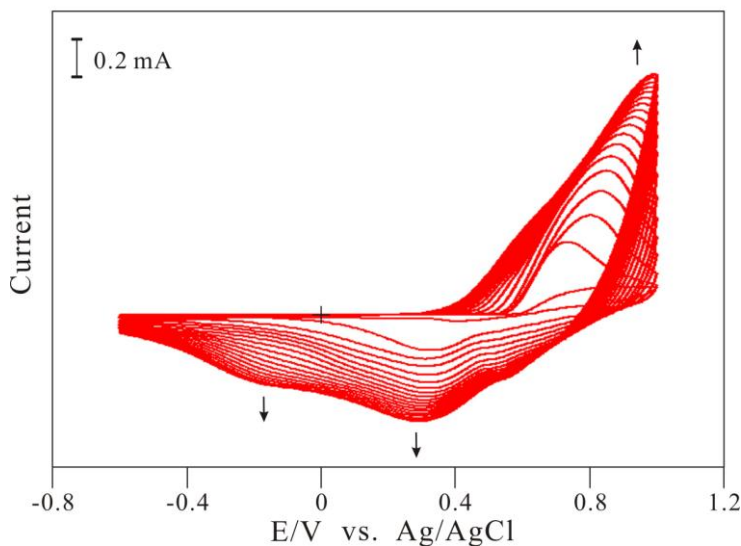


Figure 1. Cyclic voltammograms of MnO_2 -PEDOT deposition using GCE in 0.1 M LiClO_4 solution containing 5×10^{-3} M hydroxyl propyl- β -cyclodextrin, 0.01 M EDOT, and 0.1 M manganese (II) acetate. Scan rate = 0.1 Vs^{-1} .

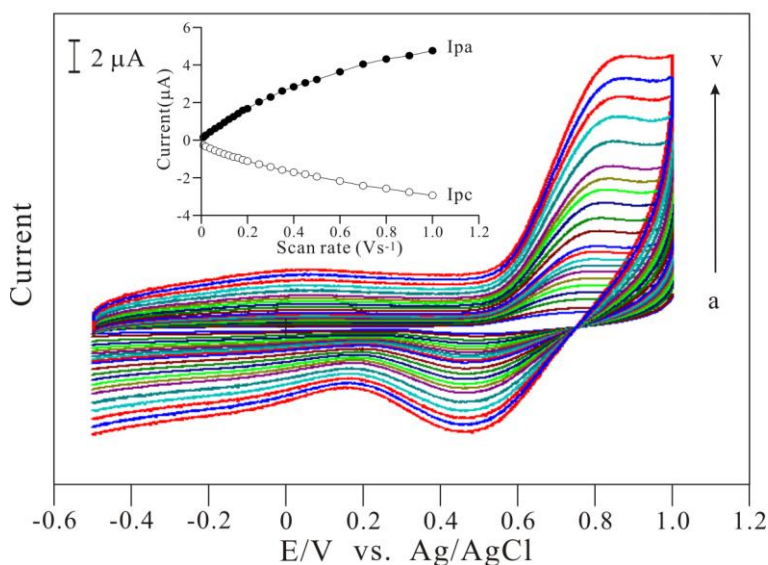


Figure 2. Cyclic voltammograms of MnO_2 -PEDOT/GCE examined in NaOH buffer solution (pH 10.4) with various scan rates of (a) 0.01, (b) 0.02, (c) 0.04, (d) 0.06, (e) 0.08, (f) 0.1, (g) 0.12, (h) 0.14, (i) 0.16, (j) 0.18, (k) 0.2, (l) 0.25, (m) 0.3, (n) 0.35, (o) 0.4, (p) 0.45, (q) 0.5, (r) 0.6, (s) 0.7, (t) 0.8, (u) 0.9, and (v) 1 Vs^{-1} , respectively. Inset shows the plot of redox peak currents (I_{pa} and I_{pc}) vs. scan rate.

It displayed that the manganese was further oxidized to form manganese oxide on the electrode surface. Hence the MnO_2 -PEDOT hybrid film was successfully fabricated on electrode surface. The MnO_2 -PEDOT hybrid film modified GCE was slightly washed with deionized water to further study.

The MnO_2 -PEDOT/GCE was employed in pH 7 PBS for the different scan rate studies. Fig. 2 showed the cyclic voltammograms of MnO_2 -PEDOT hybrid film examined in pH 7 PBS with various scan rates. Both anodic and cathodic peak currents (I_{pa} & I_{pc}) were increasing with the increase of scan rate.

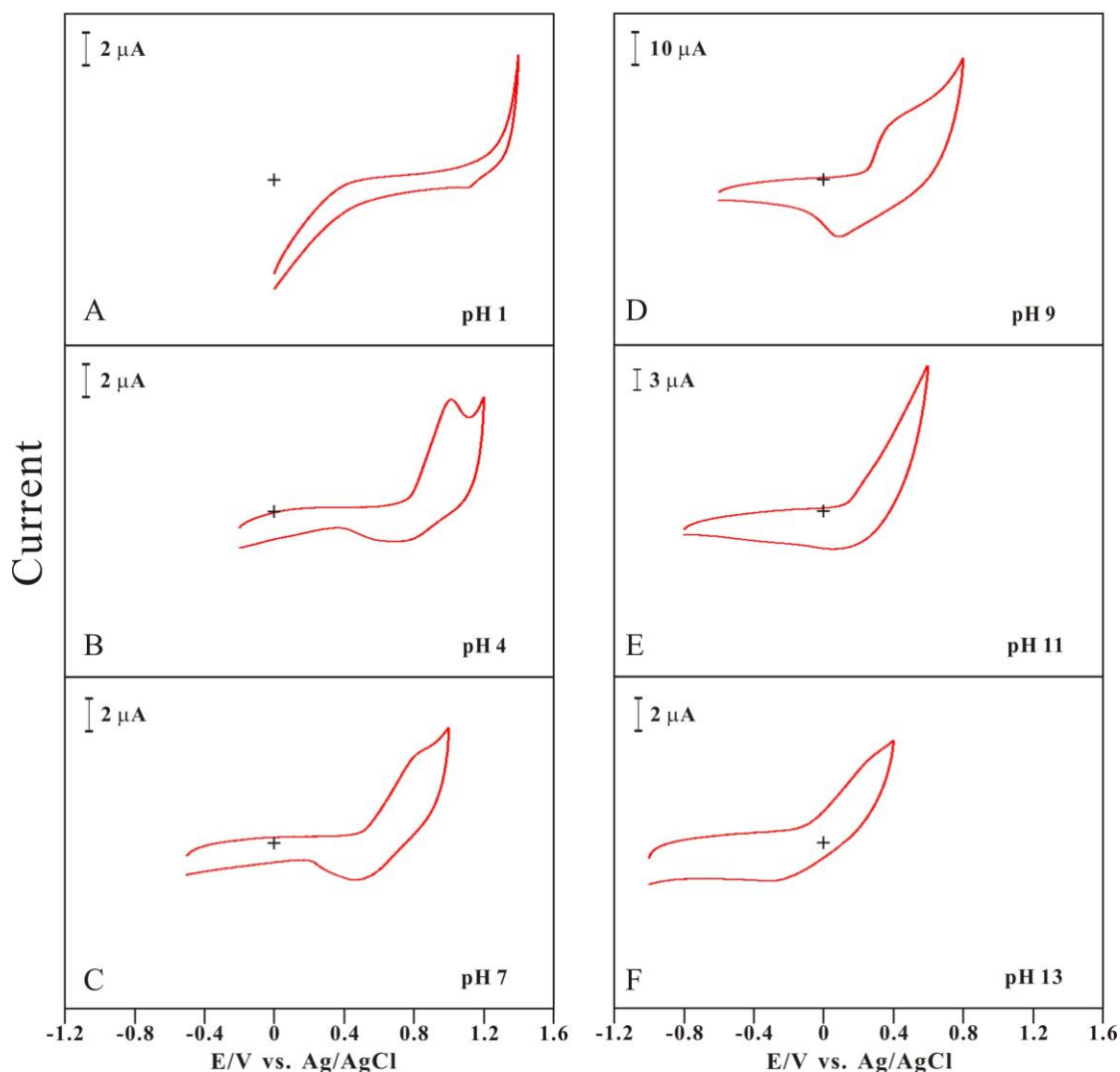


Figure 3. Cyclic voltammograms of MnO_2 -PEDOT/GCE examined in various pH conditions of (A) pH 1, (B) pH 4, (C) pH 7, (D) pH 9, (E) pH 11, and (F) pH 13, respectively. Scan rate = 0.1 Vs^{-1} .

They were directly proportional to scan rate ($0.01 - 0.1 \text{ Vs}^{-1}$) depicted the diffusion-less process. This composite was surface-confined on electrode surface. By the way, the background current in the potential range of $-0.5 - 0.6 \text{ V}$ was also found increasing with the increase of scan rate. This proved that the conducting polymer PEDOT existed in the hybrid film with higher conductivity.

Here in the neutral pH condition the proposed film exhibited as a quasi reversible process with clearly oxidation and reduction peaks of MnO_2 and a diminished broad couple which resembles the PEDOT, respectively. Finally the MnO_2 -PEDOT hybrid film found to be electrochemically active and stable in pH 7 PBS solution, respectively. Considering the physiological pH, we selected pH 7 PBS solution for the further electrochemical studies. Before this, the MnO_2 -PEDOT hybrid film was examined in different pH solutions.

Fig. 3 showed the cyclic voltammograms of MnO_2 -PEDOT/GCE examined in different pH solution from pH 1 to 13. Different electrochemical properties were observed for MnO_2 -PEDOT hybrid film in various pH solutions. It exhibited as entirely irreversible at pH 1. Further in pH 4, 7, and 9 it clearly showed the reduction and oxidation peaks of the MnO_2 . In pH 11 and 13, it displayed like a quasi reversible with the diminished electrochemical response. Therefore, pH 4, 7, and 9 buffer conditions were found to be more suitable for the electrochemical activity of the proposed film particular in pH 7. It can be concluded that the neutral pH was suitable condition for the active MnO_2 -PEDOT film.

3.2. AFM analysis of MnO_2 -PEDOT/GCE

The surface morphology of the MnO_2 -PEDOT film was examined using AFM. Here the AFM studies could furnish the comprehensive information about the surface morphology of MnO_2 -PEDOT film on the ITO surface. The AFM parameters were evaluated for 3307 nm \times 3307 nm surface area. The surface morphology of MnO_2 -PEDOT film was examined by using the tapping mode (Fig. 4).

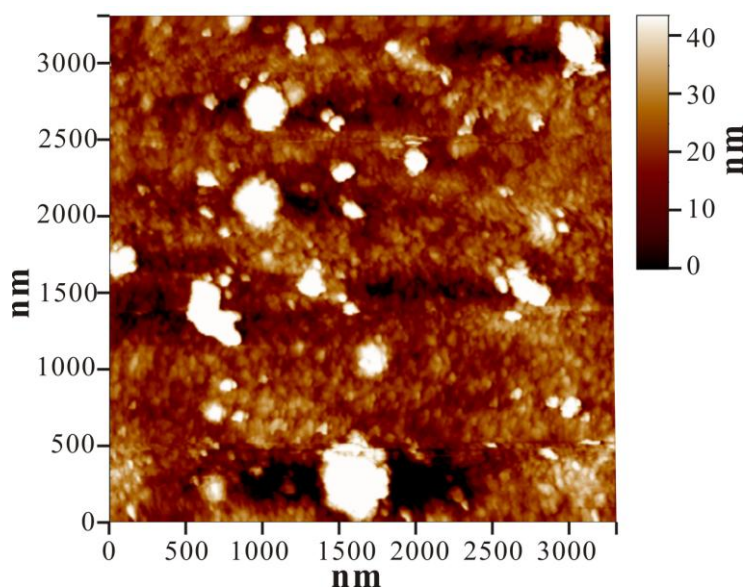


Figure 4. Tapping mode AFM image of MnO_2 -PEDOT film on ITO substrate.

From the Fig. 4, it might prove the existence of MnO_2 particles in the obvious manner along with the deposition of PEDOT. Further the other amplitude parameters such like the roughness average

(R_a) for MnO_2 -PEDOT film ($3307 \text{ nm} \times 3307 \text{ nm}$) was found as 7.04 nm . The root mean square roughness (R_{RMS}) was found as 9.04 nm . Further using the combination of skewness and kurtosis values, it identified the film surface with the relatively flat top and deep valleys. The skewness (R_{sk}) measured the symmetry of variation of the surface about its mean plane. Here the positive skewness value (0.04) obtained for MnO_2 -PEDOT film showed that the surface comprised of disproportionate number of peaks which indicated that the MnO_2 particles were unevenly allocated on the GCE surface. Next, the kurtosis (R_{ku}) was a measure of the unevenness or sharpness of the surface. A centrally distributed surface had a kurtosis value greater than 3. In this film, the kurtosis value was found as 3.44. In particular, the maximum number of MnO_2 particles had been found in the size range of 258 nm . Finally the above AFM results clearly illustrated the surface nature of the MnO_2 -PEDOT film on the GCE.

3.3. EIS analysis of MnO_2 -PEDOT/GCE

The electrochemical activity of the MnO_2 -PEDOT film modified GCE has been compared with only PEDOT modified and bare GCE using EIS technique. Impedance spectroscopy was an effective method to probe the features of surface modified electrodes. This study was employed to analyze the electrochemical activities of modified electrode with individual or mixed components. Here the complex impedance presented as a sum of the real, $Z_R(\omega)$, and imaginary $Z_I(\omega)$, components that originate mainly from the resistance and capacitance of the cell. From the shape of an impedance spectrum, the electron-transfer kinetics and diffusion characteristics was extracted.

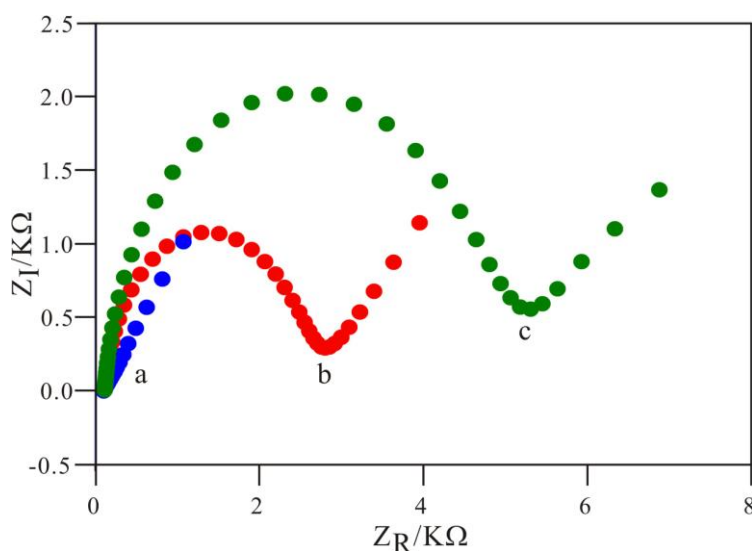


Figure 5. Electrochemical impedance spectra curves including (a) PEDOT/GCE, (b) bare GCE, and (c) MnO_2 -PEDOT/GCE examined in pH 7 PBS containing $5 \times 10^{-3} \text{ M}$ $[\text{Fe}(\text{CN})_6]^{3-}$.

Here Fig. 5 showed the Faradaic impedance spectra, presented as Nyquist plots (Z_R vs. Z_I) for the only PEDOT, bare and MnO_2 -PEDOT film modified GCE, respectively. Here the PEDOT

modified GCE exhibited almost a straight line (line a) represented the characteristics of diffusion limited fast electron-transfer process on the electrode surface. At the same time, bare GCE (curve b) showed a depressed semicircle with an interfacial resistance due to the electrostatic repulsion between the charged surface and probe molecule $\text{Fe}(\text{CN})_6^{3-/4-}$. This depressed semi circle ($R_{\text{et}} = 2.7 \text{ (Z}_R/\text{K}\Omega)$) clearly indicated the higher electron transfer resistance behavior before modifying electrode surface with PEDOT film. At the same time, the R_{et} of MnO_2 -PEDOT film modified GCE had been found as 5.3 ($\text{Z}_R/\text{K}\Omega$). Here the electron transfer resistance (R_{et}) was increased due to the deposition of MnO_2 and PEDOT as a hybrid on the GCE surface. Thus, the electron transfer process was a slow process on the MnO_2 -PEDOT film modified GCE. Also, the roughness value was increasing automatically due to the presence of MnO_2 particles in the film. This was also the specific reason for the increase of R_{et} . Finally, these results clearly illustrated the electrochemical activity of MnO_2 -PEDOT film modified GCE.

3.4. Electrocatalytic oxidation of memantine hydrochloride by MnO_2 -PEDOT/GCE

The electrocatalytic oxidation of memantine hydrochloride was investigated by MnO_2 -PEDOT/GCE.

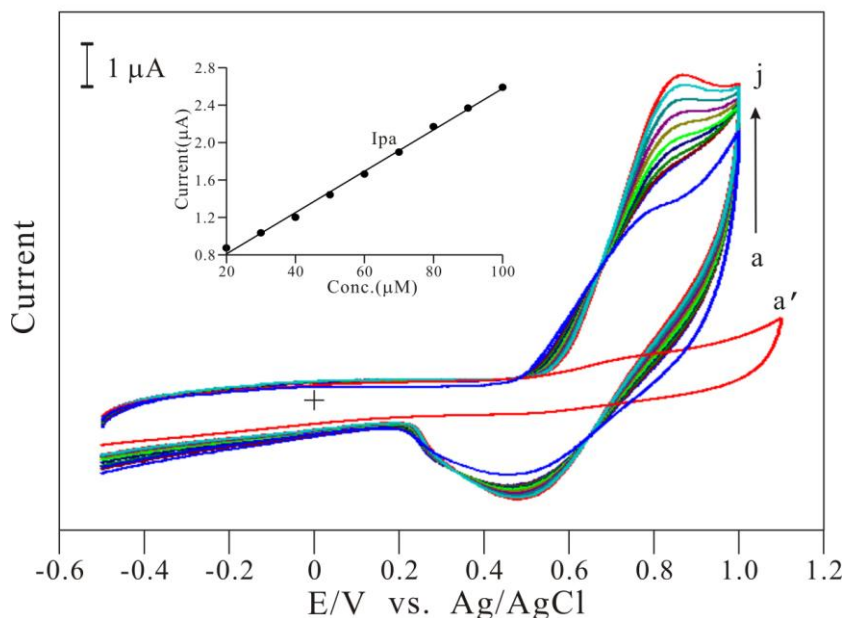


Figure 6. Cyclic voltammograms of MnO_2 -PEDOT/GCE examined in pH 7 PBS containing [memantine] = (a) 0, (b) 20, (c) 30, (d) 40, (e) 50, (f) 60, (g) 70, (h) 80, (i) 90, and (j) 100 μM , respectively. Scan rate = 0.1 Vs^{-1} . Inset shows the plot of anodic peak current (I_{pa}) vs. memantine concentration.

Fig. 6 showed the cyclic voltammograms of MnO_2 -PEDOT/GCE examined in pH 7 PBS with different concentration of memantine hydrochloride. In the scan range of 0.8 – 1.1 V, the MnO_2 -

PEDOT/GCE (curve b-v) exhibited the electrocatalytic oxidation peak at 0.81 V while the bare GCE (curve a') exhibited no oxidation peak to memantine hydrochloride concentration of 20 – 100 μM . The electrocatalytic oxidation current to memantine hydrochloride was found linearly in the range of 20 – 100 μM . This increasing peak current for memantine hydrochloride oxidation confirmed that the presence of MnO_2 particles along with the polymer possessed the higher catalytic activity for the memantine hydrochloride oxidation process. From this result, it was evident that the presence of MnO_2 particles increased the electrocatalytic activity of the film and acted as active centers for the proposed hybrid film. Therefore, the MnO_2 -PEDOT hybrid film can be the suitable material to transfer the electron between memantine hydrochloride and electrode surface. Furthermore from the current vs. calibration plot (inset of Fig. 6), the linear regression equation for this concentration range was obtained as $I_{\text{pa}}(\mu\text{A}) = 0.019C(\mu\text{M}) + 0.543$ with the correlation coefficient of $R^2 = 0.969$. Finally, this result proved the efficiency of MnO_2 -PEDOT hybrid film for the significant detection of memantine hydrochloride.

3.5. Electro catalytic oxidation of H_2O_2 by MnO_2 -PEDOT/GCE

To examine the electroanalytical performance of MnO_2 -PEDOT/GCE for H_2O_2 oxidation, the cyclic voltammetry was employed.

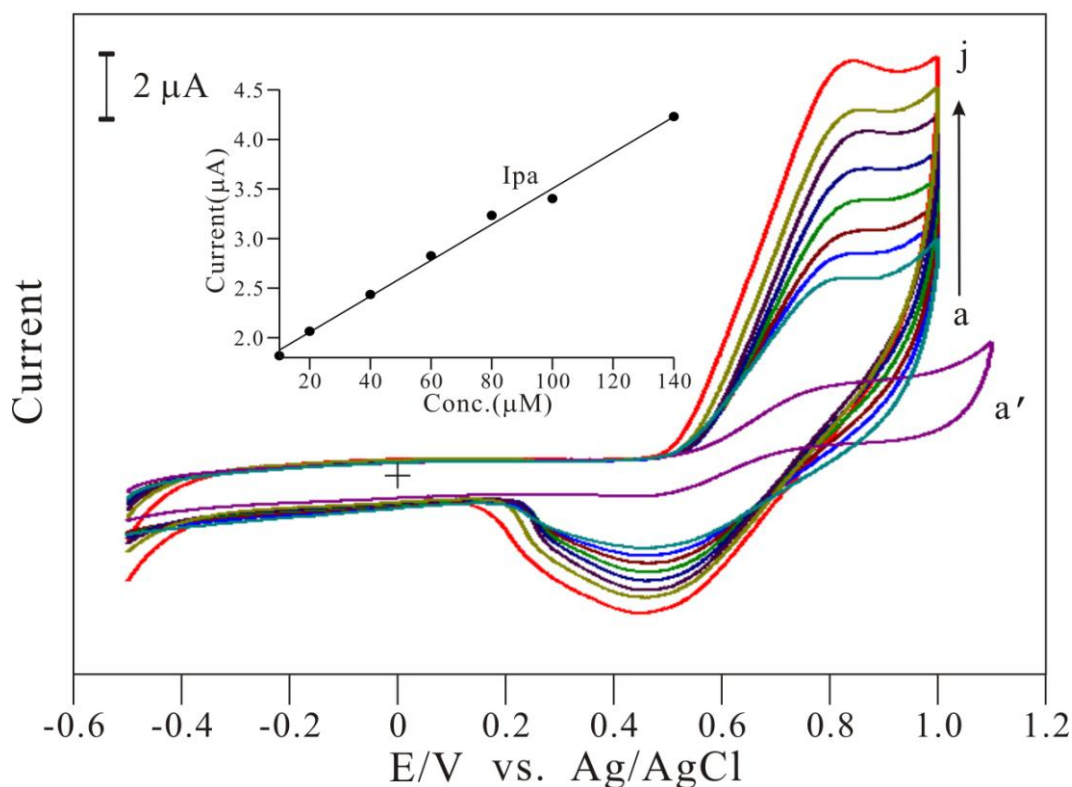


Figure 7. Cyclic voltammograms of MnO_2 -PEDOT/GCE examined in pH 7 PBS containing $[\text{H}_2\text{O}_2] =$ (a) 0, (b) 10, (c) 20, (d) 40, (e) 60, (f) 80, (g) 100, and (h) 140 μM , respectively. Scan rate = 0.1 Vs^{-1} . Inset shows the plot of anodic peak current (I_{pa}) vs. H_2O_2 concentration.

Fig. 7 showed the cyclic voltammograms of MnO₂-PEDOT/GCE examined with different H₂O₂ addition in pH 7 PBS. Here curve a' represents the oxidation process of H₂O₂ (140 μM) on bare GCE. There was no obvious peak observed for H₂O₂ oxidation at bare GCE. At the same time, the electrocatalytic oxidation current of H₂O₂ was found at 0.8 V with high current response. Here the H₂O₂ oxidation current was found linearly increasing in the range of 10-140 μM. The enhanced oxidation peak current of H₂O₂ clearly indicates the electrocatalytic oxidation process of MnO₂-PEDOT/GCE. Further the calibration plot for the H₂O₂ oxidation (inset of Fig. 7) and the linear regression equation for the detection of memantine was expressed as $I_{pa} (\mu A) = 18C(\mu M) + 1.698$ with correlation coefficient of $R^2 = 0.998$. From this result, it was found that the proposed hybrid film is suitable for the electrocatalytic oxidation of H₂O₂.

4. CONCLUSION

In this work we have successfully constructed MnO₂-PEDOT hybrid film on electrode surface by using cyclic voltammetry. The MnO₂-PEDOT hybrid film was characterized using cyclic voltammetry, AFM, and EIS analysis. In the proposed hybrid film, the MnO₂ particles were found in the size range of 258 nm. Here the presence of MnO₂ particles exhibited as active centers of the film. Further the MnO₂-PEDOT hybrid film modified GCE successfully showed efficient electrocatalytic oxidation peak for the detection of memantine hydrochloride and H₂O₂, respectively. Finally the typical application of MnO₂-PEDOT hybrid film has potential for the successful determination of memantine hydrochloride.

ACKNOWLEDGEMENTS

This work was supported by the National Science Council of Taiwan (ROC).

References

1. S. Rossi, editor. Australian Medicines Handbook 2006. Adelaide: Australian Medicines Handbook; 2006.
2. H.W. Querfurth, F.M. LaFerla, *N. Engl. J. Med.* 362 (2010) 329–344.
3. G. Aliev, M.A. Smith, J.C. de la Torre, G. Perry, *Mitochondrion* 4 (2004) 649–663.
4. J.C. de la Torre, *Lancet Neurol.* 3 (2004) 184–190.
5. M.A. Korolainen, T.A. Nyman, T. Aittokallio, T. Pirttila, *J. Neurochem.* 112 (2010) 1386–1414.
6. A. Aguzzi, T. O'Connor, *Nat. Rev. Drug Discov.* 9 (2010) 237–248.
7. F. Panza, V. Solfrizzi, V. Frisardi, B.P. Imbimbo, C. Capurso, A. D'Introno, A.M. Colacicco, D. Seripa, G. Vendemiale, A. Capurso, A. Pilotto, *Aging Clin. Exp. Res.* 21 (2009) 386–406.
8. M. Gralle, M.G. Botelho, F.S. Wouters, *J. Biol. Chem.* 284 (2009) 15016–15025.
9. S.A. Areosa, F. Sherriff, R. McShane, *Cochrane Database Syst Rev* 3 (2005) CD003154-.
10. Y. Higashi, S. Nakamura, H. Matsumura, Y. Fujii, *Biomed. Chromatogr.* 20 (2006) 423–428.
11. N. Reichová, J. Pazourek, P. Polás̃ková, J. Havel, *Electrophoresis* 23 (2002) 259–262.
12. M.Y. Liu, S.N. Meng, H.Z. Wu, S. Wang, M.J. Wei, *Clin. Ther.* 30 (2008) 641–653.

13. A.A. Almeida, D.R. Campos, G. Bernasconi, S. Calafatti, F.A.P. Barros, M.N. Eberlin, E.C. Meurer, E.G. Paris, J. Pedrazzoli, *J. Chromatogr. B* 848 (2007) 311–316.
14. S. Thiagarajan, S.-M. Chen, *J. Solid State Electr.* 13 (2009) 445-453.
15. S. Thiagarajan, B.-W. Su, S.-M. Chen, *Sensor Actuat B-Chem.* 136 (2009) 464-471.
16. T.-H. Tsai, S. Thiagarajan, S.-M. Chen, *Electroanal.* 22 (2010) 680-687.
17. Y. Usui, K. Sato, M. Tanaka, *Angew. Chem. Int. Ed.* 42 (2003) 5623-5625.
18. E.A. Mazziio, K.F.A. Soliman, *J. Appl. Toxicol.* 24 (2004) 99-106.
19. M. Zayats, R. Baron, I. Popov, I. Willner, *Nano Lett.* 5 (2005) 21-25.
20. P.A. Tanner, A.Y.S. Wong, *Anal. Chim. Acta* 370 (1998) 279-287.
21. N.V. Klassen, D. Marchington, H.C.E. McGovan, *Anal. Chem.* 66 (1994) 2921-2925.
22. O.S. Wolfbeis, A. Durkop, M. Wu, Z. Lin, *Angew. Chem. Int. Ed.* 41 (2002) 4495-4498.
23. X. Shu, Y. Chen, H. Yuan, S. Gao, D. Xiao, *Anal. Chem.* 79 (2007) 3695-3702.
24. U. Pinkernell, S. Effkemann, U. Karst, *Anal. Chem.* 69 (1997) 3623-3627.
25. S.A. Kumar, S.M. Chen, *Talanta* 72 (2007) 831-838.
26. T.H. Tsai, S. Thiagarajan, S.-M. Chen, *Intl. J. Electrochem. Sci.*, 6 (2011) 3878-3889.
27. S. Thiagarajan, T.H. Tsai, S.-M. Chen, *Intl. J. Electrochem. Sci.*, 6 (2011) 2235-2245.
28. S.L. Brock, N. Duan, Z.R. Tian, O. Giraldo, H. Zhou, S.L. Suib, *Chem. Mater.* 10 (1998) 2619-2628.
29. S.I. Córdoba De Torresi, A. Gorenstrein, *Electrochim Acta* 37 (1992) 2015-2019.
30. V. Parra, A.A. Arrieta, J.A. Fernandez-Escudero, H. Garcia, C. Apetrei, M.L. Rodriguez-Mendez, J.A. Saja, *Sens. Actuators B* 115 (2006) 54–61.
31. L. Pigani, G. Foca, K. Ionescu, V. Martina, A. Ulrici, F. Terzi, M. Vignali, C. Zanardi, R. Seeber, *Anal. Chim. Acta* 614 (2008) 213-222.
32. L. Agüi, P. Yáñez-Sedeño, J.M. Pingarrón, *Electroanalysis* 9 (1997) 468-473.
33. P.G. Pickup, *Mod. Aspects Electrochem.* 33 (1999) 549-597.
34. J. K. Chang, W.T. Tsai, *J. Electrochem. Soc.* 150 (2003) A1333-A1338.
35. M.S. Wu, P.C. Chiang, *J. Electrochem. Solid-State Lett.* 7 (2004) A123-A126.
36. J. Desilvestro, O. Haas, *J. Electrochem. Soc.* 137 (1990) C5-C22.
37. L.B. Groenendaal, G. Zotti, P.H. Aubert, S.M. Waybright, J.R. Reynolds, *Adv. Mater.* 15 (2003) 855-879.
38. R. Liu, F. Oba, E.W. Bohannan, F. Ernst, J.A. Switzer, *Chem. Mater.* 15 (2003) 4882-4885.
39. M.J. Siegfried, K.S. Choi, *J. Am. Chem. Soc.* 128 (2006) 10356-10357.
40. C.X. Ji, P.C. Searson, *Appl. Phys. Lett.* 81 (2002) 4437-4439.
41. S.I. Cho, W.J. Kwon, S.J. Choi, P. Kim, S.A. Park, J. Kim, S.J. Son, R. Xiao, S.H. Kim, S.B. Lee, *Adv. Mater.* 17 (2005) 171-175.
42. V.S. Vasantha and S.M. Chen, *J. Electroanal. Chem.*, 592 (2006) 77-87.
43. V.S. Vasantha and S.M. Chen, *Electrochim. Acta*, 51 (2005) 347-355.
44. S. M. Chen, K. T. Peng, *J. Electroanal. Chem.* 547 (2003) 179.
45. S.M. Chen, K.C. Lin, *J. Electroanal. Chem.* 523 (2002) 93.
46. S. M. Chen, W. Y. Chzo, *J. Electroanal. Chem.*, 587(2006) 226.
47. K. C. Lin, C. Y Yin, S. M. Chen, *Int. J. Electrochem. Sci.* 6 (2011) 3951.